Formation of thallium islands on the Si(111)-7×7 surface

N. D. Kim, C. G. Hwang, and J. W. Chung*
Physics Department and Basic Science Research Institute, Pohang University of Science and Technology, San 31 Hyoja Dong, Pohang 790-784, Korea

T. C. Kim and D. Y. Noh
Department of Materials Science and Engineering, Gwangju Institute of Science and Technology, Gwangju, Korea
(Received 26 October 2004; revised manuscript received 11 March 2005; published 19 July 2005)

We have studied the formation of thallium (Tl) islands on the Si(111)-7×7 surface by utilizing synchrotron x-ray scattering. The Si substrate is found to maintain its 7×7 periodicity until metastable Tl islands of three different morphologies grow to their maximum size at room temperature. Analysis of several Bragg reflections from these Tl islands reveals that the three different types of Tl islands having different thermal stability can be characterized by their unique basal planes—(001), (100), and (101). Upon increasing the Tl dose the most abundant islands with a basal plane of (001) grow their lateral size up to a limiting value of 38 nm while their lattice parameter approaches a bulk value of 0.2996 nm. We interpret our data primarily in terms of strain-limited growth of the Stranski-Krastanov type.

DOI: 10.1103/PhysRevB.72.035338 PACS number(s): 61.10.Nz, 68.43.Fg, 68.47.Fg, 68.18.Jk

Understanding the growth mechanism of self-assembled thin films or islands on crystalline substrates has been a subject of extensive research efforts.[1] All the processes involved, such as deposition of adsorbates, surface diffusion, nucleation, and aggregation of small islands, have to be investigated on the atomic level in order to control the shape, size, and ordering of nanoscale islands.[2,3] Growth of epitaxial nonreactive metallic islands, where surface and interface energies compete to form an equilibrium structure, can be described by a scaling law showing that the size and the number density of islands depend on powers of adsorbate coverage or deposition time.[1] One often finds, however, that the scaling laws may be violated when particular physical origins such as anisotropic strains,[4] surface defects,[5] electronic effects,[6] and quantum size effects[7] dominate. In particular, the strain plays a crucial role in self-assembled quantum dots by stimulating the detachment of edge atoms to cause a narrow size distribution.[8–10]

Nonreactive systems such as Ag, Pb, In, Tl, and Al on semiconductors[5–7,11–20] have been of interest as prototypical examples in understanding the atomistic processes in heteroepitaxial growth. For the Tl/Si(111) system, in particular, Vitali *et al.*[19] reported that the growth of Tl on a Si(111)-7×7 surface at room temperature (RT) followed the Stranski-Krastanov mode with a two-monolayer (ML) thick wetting layer. [For Si(111), 1ML=7.8×10^{14} atoms/cm^2] Additional Tl adatoms beyond the wetting layer are reported to form large three-dimensional islands which do not easily coalesce upon further dosing. The number density of dropletlike Tl islands is small, and the islands are largely separated.[14,19] Similarly, large Tl islands are reported to form on a Tl-induced Si(111)-1×1 surface.[20]

In this study, we have investigated the growth of Tl islands on the Si(111)-7×7 at RT as a function of Tl dose as well as annealing temperature. We find that the Tl islands formed are significantly different from those nucleated on the wetted Tl/Si(111)-1×1 surface. We also observe that the strain energy associated with substrate reconstruction plays a crucial role in the nucleation and morphology of islands grown.

Figure 1(a) schematically depicts the three different types of Tl islands observed on the Si(111)-7×7 surface at RT. These islands are identified by their characteristic basal planes (001), (100), and (101), respectively. We have measured several reflections from these islands with H and K indices for in-plane reflections and the index L for out-of-plane reflections. The subscripts 1, 2, and 3 conveniently denote the islands of basal planes, (001), (100), and (101) planes, respectively. Figure 1(b) shows the positions of in-plane Bragg reflections obtained from these islands and Si substrate by using grazing-incidence synchrotron x-ray diffraction.

We have adopted a custom-designed ultrahigh-vacuum (UHV) x-ray scattering chamber, which was mounted on a four-circle diffraction goniometer (2+2 mode) at the 5C2

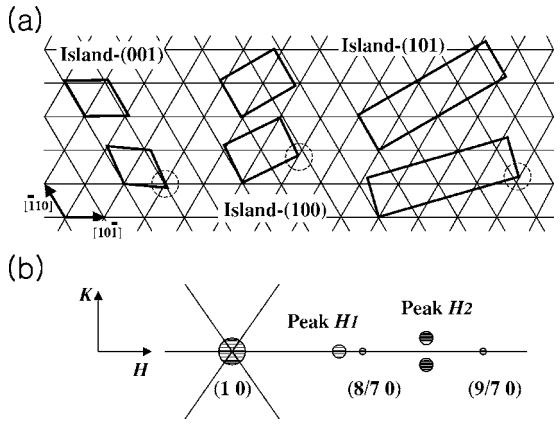

FIG. 1. (a) Schematics of the three different types of Tl islands characterized by basal planes of (001), (100), and (101) on a hexagonal lattice. Upper (lower) unit cells represent the islands aligned (rotated) with respect to the symmetry direction [$\bar{1}$10]. Details are described in text. (b) In-plane reflections observed at $L\simeq0$. The (1 0), (8/7 0), and (9/7 0) reflections are from the Si substrate and reflections denoted as H_1 and H_2 are from Tl islands.

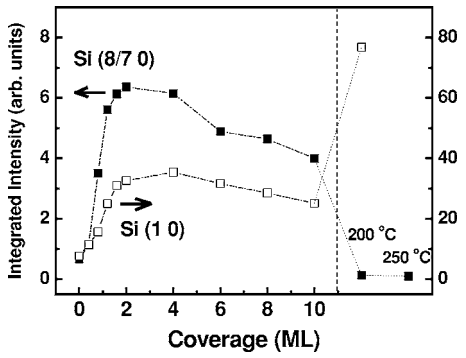

FIG. 2. Evolution of the integrated intensities of the Si(1 0) and (8/7 0) reflections with increasing Tl dose. The vertical dotted line separates data points without (left) and with (right) annealing.

K-JIST beamline of the Pohang Light Source in Korea.[21] The technical details of the x-ray scattering chamber and the goniometer used have been described elsewhere.[22] The synchrotron beam size with a wavelength of 1.23 Å and the detector slits provided a resolution function with the full width at half maximum (FWHM) less than 0.001 $Å^{-1}$. The base pressure of the chamber was maintained below 3×10^{-10} Torr during the entire measurements. The Si sample was cleaned by repeated degassing at 600 °C with frequent flashing up to 1200 °C followed by annealing at 850 °C. The sample cooled slowly down to RT after such a cleaning process produced a well-defined 7×7 surface. We have confirmed the cleanliness of the sample by routinely measuring a series of seventh-order reflections from the clean 7×7 surface. The reciprocal lattice unit vectors (in the unit of $Å^{-1}$) are defined as $\mathbf{b}_1 \| [11\bar{2}]$, $\mathbf{b}_2 \| [\bar{1}10]$, and $\mathbf{b}_3 \| [111]$. The momentum transfer $\mathbf{q}$ is then defined by $\mathbf{q} = H\mathbf{b}_1 + K\mathbf{b}_2 + L\mathbf{b}_3$.

After cleaning the sample by the process mentioned above, Tl atoms were deposited on the clean 7×7 surface at RT. Intensities of an integral-order reflection Si(1 0) and a fractional-order reflection Si(8/7 0) from the substrate silicon surface have been monitored during deposition as shown in Fig. 2. One notes that the intensities of both reflections increase rather quickly with increasing Tl dose at the early stage and then reach maxima near 2 ML indicating the completion of two-dimensional wetting layers as noted in a previous study.[19] The decrease of intensities for both reflections upon further dose (dose rate of about 0.4 ML/min) is apparent due to the formation of Tl islands as described below. We find that the Tl islands begin to form at about 1.0 ML where the wetting layers are not yet completed (not shown). This is seen by the fact that the characteristic Tl reflections begin to appear at 1.0 ML even though their intensities are extremely weak. An interesting observation is that the Si(8/7 0) reflection disappears completely while the Si(1 0) becomes stronger upon annealing at 300 °C for several minutes, which is ascribed to the transformation of the substrate surface from the 7×7 phase to the 1×1 phase.[21]

In Fig. 3, we have presented our in-plane H scans along the Si(1 0) direction and out-of-plane L scans along the surface normal beyond the Bragg reflection (111) of the silicon substrate as a function of Tl dose and of annealing temperature. The reflections H_1 or H_2 are found to appear near 1.0 ML, and then grow in intensity with increasing Tl dose almost linearly up to 6.0 ML [see solid line in Fig. 5(a)]. As schematically shown in Fig. 1 for the sitting of the islands with respect to the silicon substrate, the (001)-based islands are formed mostly in parallel to the symmetry direction ($[\bar{1}10]$) of the hexagonal surface, while the (100)-based islands are slightly rotated by 2.03° with respect to the symmetry direction as seen from the transverse scans of H_2 in Fig. 3 (bottom right). As mentioned earlier, the presence of such islands is distinctly different from Tl islands formed on the 1×1 surface where islands with a basal plane (001) are rotated by ~8.5° with respect to the symmetry direction.[20]

In order to characterize the morphology of the three different types of Tl islands with respect to the substrate more accurately, we have carefully performed an *ex situ* measurement with the sample deposited more than 30 ML at RT. Our ϕ scans of Tl Bragg reflections are shown in Fig. 4. For the (101)-based islands, the Tl(002) Bragg reflection inclined by 61.5° from the surface normal is found at azimuthal angles rotated by 14° off from the symmetry direction. The Tl(101) Bragg reflection for the (001)-based islands is observed at both 0° and 3.1° with respect to the symmetry direction. Comparison of intensities of these reflections suggests that the rotated islands appearing at 3.1° are populated much less than 3% of the aligned ones at 0°. The presence of the 2° rotation of the (100)-based islands has been confirmed by observing the Tl(101) Bragg reflection inclined by 28.5° off from the specular direction (not shown). These observations led us to identify the Tl islands formed on the Si(111)-7 $\times 7$ surface at RT by the three different basal planes (001), (100), and (101) as mentioned earlier.

The thermal stability of the Tl islands has been studied by annealing the sample at several elevated temperatures. Upon annealing at 200 °C for several minutes, the (001)-based islands apparently grow while the (100)-based islands quickly shrink as indicated by the enhanced intensity of H_1 in sharp contrast to the nearly disappeared H_2 (or L_2) in Fig. 3. When annealed at 250 °C, however, the (101)-based islands grow at the expense of the (001)-based islands as seen by the significantly reduced H_1 (or L_1) compared to the much enhanced L_3. All the islands disappear completely upon annealing at 300 °C. It seems quite surprising to find that the (101)-based islands of least symmetry are thermally more stable than the other islands of higher symmetry. Although a microscopic picture explaining such unusual thermal behavior is absent at present, this may be reasonably understood when one considers the strain energy associated with the lattice mismatch and their symmetry.[16]

We now try to explain the presence of such rotated Tl islands by considering a purely geometrical row-matching condition for a minimum misfit as done similarly for the "8×8" Pb on the Si(111)-7×7 at RT.[12] Assuming that all Tl atoms sit in the corrugation potential ditches with a nearest-neighbor distance in the first Tl layer $a_0 = 3.36$ Å $\left(= 3.84 \text{ Å} \times \frac{7}{8}\right)$ as done earlier,[12] one may calculate the angles rotated under the condition that at least one side of each unit cell of the islands is matched on the symmetry row of the hexagonal lattice, as indicated by dotted circles in Fig. 1(a). The increase of the Si(8/7 0) reflection with Tl dose, in fact,

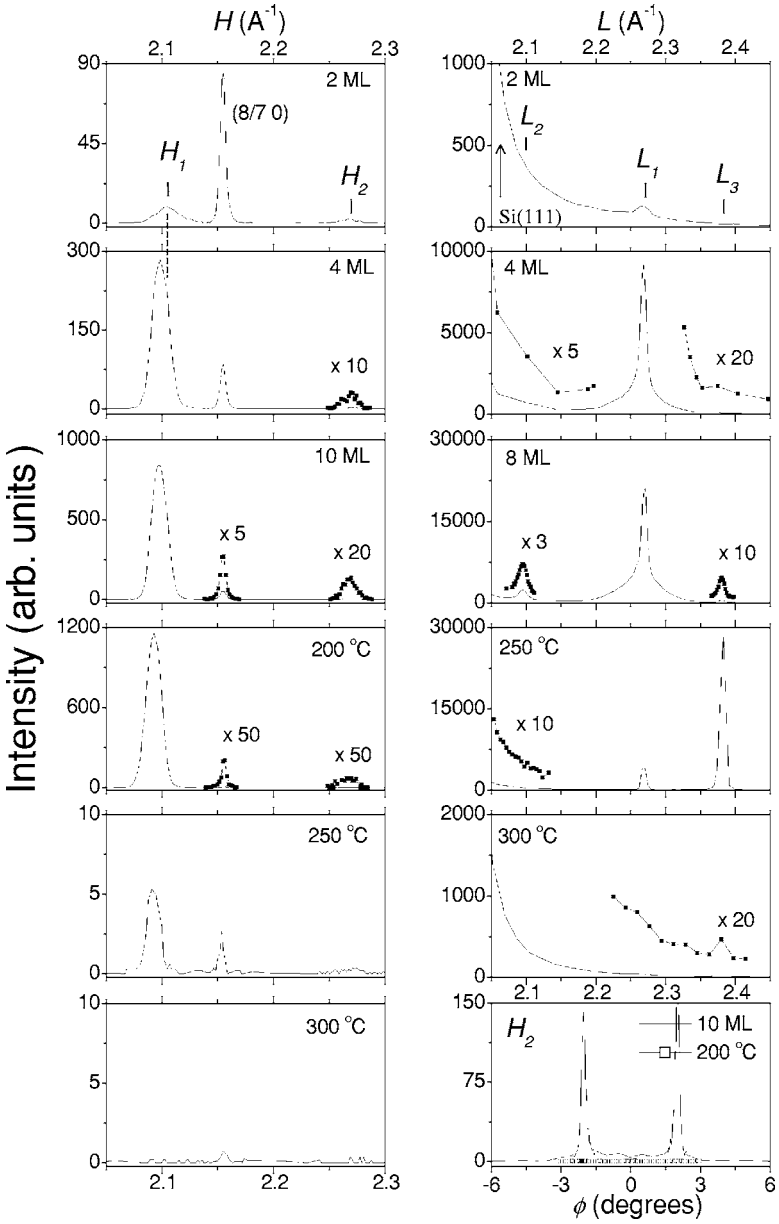

FIG. 3. A series of scans showing changes as a function of Tl dose and of annealing temperature. In-plane H scans (out-of plane L scans) are plotted in the left (right) side. The last plot in the bottom right shows transverse (ϕ) scans of H_2. Note that H_1 shifts slightly from its position at 2 ML as marked by the vertical dotted line in the top left.

supports such an assumption. We obtain an angle of 1.8° for the (100)-based islands with a rectangular unit cell (3.46×5.52 Å^2), which matches well with our experimental value of 2.03°. Similarly we obtain 14.0° and 2.8° for the (101)- and (001)-based islands, respectively. These angles also match quite well with those observed angles 14.00° and 3.10°, respectively (see Fig. 4) for the rectangular unit cell (3.46×12.56 Å^2) of the (101)-based and the hexagonal unit cell (3.46 Å) of the (001)-based islands. We thus understand the presence of three different types of Tl island, despite the dominant population ($\geq 90\%$) of the (001) type, as the configuration to achieve a minimum energy state with reduced misfits between islands.

By considering the energy cost in the row-matching model, one may also account for the unusual thermal behavior of the Tl islands in Fig. 3. We first calculate the rotation angles required for each type of Tl island for the annealed surface where the substrate returns back to the 1×1 with a lattice constant $a_0 = 3.84$ Å. We obtain the angles 9.0°, 6.6°, and 14.7° for the (001)-,[20] the (100)-, and the (101)-based islands, respectively. One easily notices that the (101)-based islands remain almost unchanged (not rotated) by the annealing while other types of islands are required to rotate by relatively large degrees of about 6.3° for the (001)-based and 4.8° for the (100)-based islands. The high energy cost demanded to rigidly rotate the (100)- or (001)-based islands may cause those islands to disappear eventually upon annealing while the (101)-based islands survive by experiencing no or very little energy cost.

The most abundant (001)-based islands are found to grow with Tl dose as shown in Fig. 5, where the evolution with increasing Tl dose is presented for the integrated intensity (a) and the average dimensions of the islands (b). The average lateral size (empty squares) and the height (not shown) have been derived from full width at half maximum (FWHM) of H_1 and L_1, respectively. Similar data are also shown in Fig. 6

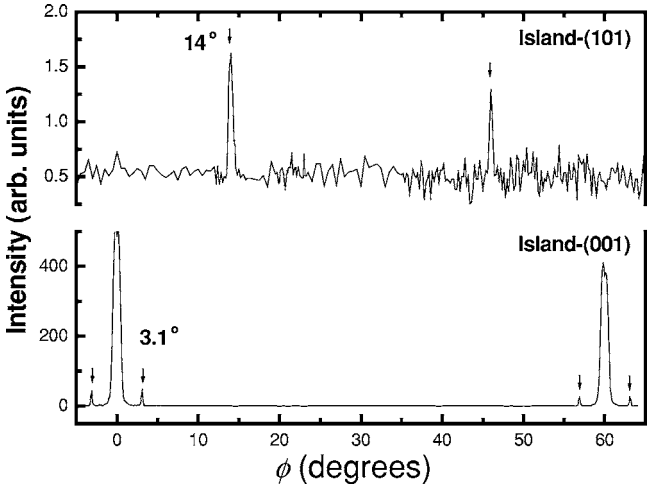

FIG. 4. *Ex situ* measurement of ϕ scans of two Tl Bragg reflections illustrating the orientation of the Tl islands. The Tl(002) Bragg reflection observed from the (101)-based islands indicates that the islands are rotated by 14° with respect to the symmetry direction. The Tl(101) Bragg reflection from the (001)-based islands is also observed at 0° and 3.1°.

for the lattice parameter obtained from the peak position of H_1.

One immediately notices that the islands grow in size rapidly with increasing Tl dose up to about 4 ML, where the islands remain almost unchanged in their size upon further dose. The fact that the integrated intensity in Fig. 5(a) continues to increase with Tl dose while the average size remains fixed above 4.0 ML [Fig. 5(b)] suggests that the number density of the islands increases with Tl dose while the average size of the islands is limited to a certain value as noticed elsewhere.[6,15] As shown in Fig. 5(b), the limited dimensions of the islands are ~38 nm and ~44 nm for the lateral size and the height, respectively.[23]

In order to understand such features, we have fitted our measured intensity of H_1 with a theoretical formula $I(q)$ assuming a Gaussian distribution for the number density of islands $n_i \approx e^{-(s_i-\langle s\rangle)^2/w^2}$. Here s_i, $\langle s\rangle$, and w are the size of the ith island, average island size, and width of the size distribution, respectively. The intensity is incoherently summed over all the islands by assuming a large separation between islands. The function $I(q)$ we used is[24]

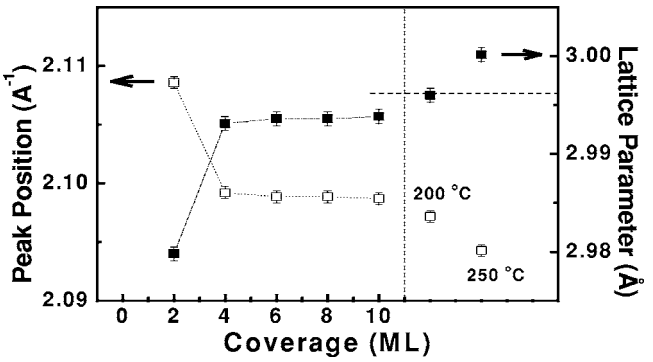

FIG. 6. Evolution of the position of H_1 and the lattice parameter with Tl dose. The horizontal dotted line indicates a bulk lattice parameter of 2.996 Å. The vertical dotted line separates data as in Fig. 2.

$$I(q) \sim P(q-q_0, w, \langle s\rangle) e^{-\langle s\rangle^2 (q-q_0)^2/[4\pi + w^2 (q-q_0)^2]},$$

where q_0 is the peak position. $P(q)$ is a polynomial function of q, w, and $\langle s\rangle$. This fit function is found to describe our data reasonably well as shown by the solid curve in Fig. 5(b) for $\langle s\rangle$. Our fit results for the (001)-based islands reveal a quite narrow distribution for the island size, i.e., $w/\langle s\rangle < 0.1$ above 4 ML. Moreover, the average island size turns out to be nearly unaffected by the size distribution itself.[25] We are thus led to believe that the variation of FWHM in Fig. 5(b) reflects faithfully the change in the average size of the islands.

It is noted that the lattice parameter also approaches the bulk value as presented in Fig. 6.[26] The average separation between neighboring islands is estimated to be about less than μm in good agreement with previous results.[19,27] We also notice that the thermally metastable islands at RT become almost completely relaxed by annealing at 200 °C. This is seen by the increased intensity with the unchanged island size (Fig. 5) as well as the lattice parameter close to that of the bulk value (Fig. 6). The dramatic changes in size accompanying the significant loss in peak intensity upon annealing at 250 °C in Fig. 5, however, reveal a different thermal response of the islands compared to that at 200 °C. At 250 °C, the islands apparently migrate more actively and agglomerate into larger ones resulting in the reduction of

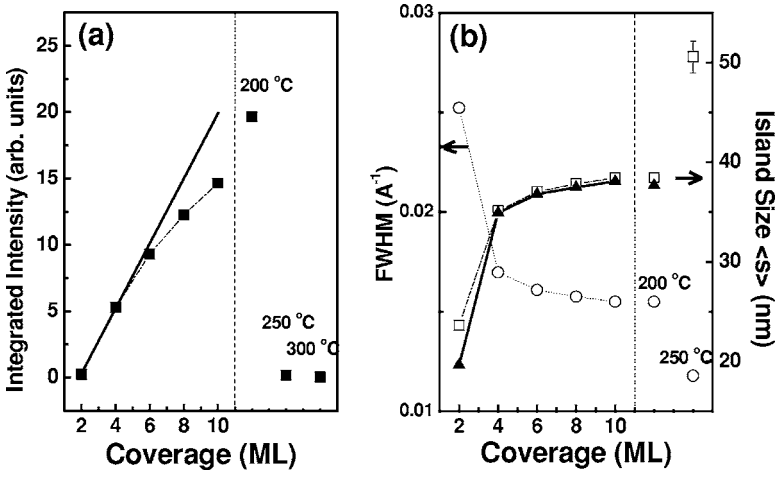

FIG. 5. (a) Integrated intensity of H_1 from the (001)-based Tl islands versus Tl dose. The solid line exhibits nearly linear growth at the initial stage of Tl adsorption. Note that the intensity saturates upon annealing at 200 °C. (b) Average island size versus Tl dose. The solid curve with data in filled triangles is a fit curve for the average size of the islands. The vertical dotted line separates data as in Fig. 2.

their number density. Such a feature can be caused partly by the substrate reconstruction back to the 1×1 surface and partly by the desorbed Tl adatoms from the surface. The data point produced by annealing at 250 °C in Fig. 6 indicating the lattice parameter slightly greater than that of the bulk value may be due to the extra defects or disorders thermally activated.

At the earlier stage of Tl dose below 2 ML, the strain due to lattice mismatch $\varepsilon[\equiv(a-a_o)/a_o]$ is estimated to be $\approx -0.5\%$, which is found to be easily relieved upon annealing at 200 °C. It has been reported that significant surface stress can reduce the lattice parameter of a small cluster as the cluster size decreases.[28] We observe a similar decrease in the lattice parameter for the (001)-based Tl islands when the island size decreases [see Fig. 5(b) and Fig. 6]. This is, however, in contrast with the lattice parameter of In islands which is independent of the island size.[14] All such examples suggest a driving force that may restrict island size formed on crystalline substrates. We believe that elastic strain caused by lattice mismatch between adlayer and substrate may be one of such driving forces.[8–10] Similar strain-induced stabilization has been reported also for the strained two-dimensional islands formed at submonolayer heteroepitaxy.[10]

In summary, we have investigated the formation of Tl islands on the Si(111)-7×7 surface at RT. We observe three distinct types of islands grown epitaxially on the wetted Tl layers in the Stranski-Krastanov mode. Interestingly, the least symmetric (101)-based islands are found to be the most stable thermodynamically surviving from the annealing at 250 °C. The most abundant (001)-based islands below 200 °C barely remain at 250 °C and the (100)-based islands disappear completely. The size of the (001)-based islands at RT grows rapidly with increasing Tl dose initially but eventually reaches a limiting value of 38 nm. We ascribe such an unusual thermal stability and the presence of a limited size of Tl islands to the strain energy cost due to the lattice mismatch between Tl adlayers and the substrate.

This work was supported in part by the X-ray/Particle-beam Nanocharacterization Program (No. RN0326). D.Y.N. acknowledges support from the Korean Science and Engineering Foundation under Grant No. R01-2002-000-00469-0.

*Electronic address: jwc@postech.ac.kr; URL: http://www.postech.ac.kr/phys/snpl/

[1] J. A. Venables, G. D. T. Spiller, and M. Hanbucken, Rep. Prog. Phys. **47**, 399 (1984); M. Zinke-Allmang, L. C. Feldman, and M. H. Grabow, Surf. Sci. Rep. **16**, 377 (1992).
[2] Z. Zhang and M. G. Lagally, Science **276**, 377 (1997).
[3] H. Brune, M. Giovannini, K. Bromann, and K. Kern, Nature (London) **394**, 451 (1998).
[4] Y.-W. Mo, R. Kariotis, D. E. Savage, and M. G. Lagally, Surf. Sci. **219**, L551 (1989).
[5] H. Hirayama, H. Okamoto, and K. Takayanagi, Phys. Rev. B **60**, 14260 (1999).
[6] D. E. Savage and M. G. Lagally, Phys. Rev. Lett. **55**, 959 (1985).
[7] K. Budde, E. Abram, V. Yeh, and M. C. Tringides, Phys. Rev. B **61**, R10602 (2000).
[8] C. Ratsch, A. Zangwill, and P. Smilauer, Surf. Sci. **314**, L937 (1994).
[9] A.-L. Barabasi, Appl. Phys. Lett. **70**, 2565 (1997).
[10] M. Meixner, E. Scholl, V. A. Shchukin, and D. Bimberg, Phys. Rev. Lett. **87**, 236101 (2001); **88**, 059901(E) (2002).
[11] J. J. Metois and G. Le Lay, Surf. Sci. **133**, 422 (1983).
[12] H. H. Weitering, D. R. Heslinga, and T. Hibma, Phys. Rev. B **45**, 5991 (1992).
[13] L. Li, C. Koziol, K. Wurm, Y. Hong, E. Bauer, and I. S. T. Tsong, Phys. Rev. B **50**, 10834 (1994).
[14] S. L. Surnev, J. Kraft, and F. P. Netzer, J. Vac. Sci. Technol. B **13**, 1389 (1995).
[15] F. P. Leisenberger, H. Ofner, M. G. Ramsey, and F. P. Netzer, Surf. Sci. **383**, 25 (1997).
[16] R. Groger, M. Barczewski, and P. von Blanckenhagen, Surf. Sci. **454–456**, 761 (2000).
[17] F. Moresco, M. Rocca, T. Hildebrandt, and M. Henzler, Surf. Sci. **463**, 22 (2000).
[18] J. M. Zuo and B. Q. Li, Phys. Rev. Lett. **88**, 255502 (2002).
[19] L. Vitali, F. P. Leisenberger, M. G. Ramsey, and F. P. Netzer, J. Vac. Sci. Technol. B **17**, 1676 (1999).
[20] L. Vitali, M. G. Ramsey, and F. P. Netzer, Surf. Sci. **452**, L281 (2000).
[21] N. D. Kim, C. G. Hwang, J. W. Chung, T. C. Kim, H. J. Kim, and D. Y. Noh, Phys. Rev. B **69**, 195311 (2004).
[22] K. W. Evans-Lutterodt and Mau-Tsu Tang, J. Appl. Crystallogr. **28**, 318 (1995).
[23] The limiting height of 44 nm is estimated from the FWHM of L_1 for a Tl dose above 4.0 ML.
[24]
$$I(q) \simeq \sum_{\text{island } j} \frac{\sin^2[s_j(q-q_0)_x/2]}{\sin^2[(q-q_0)_x/2]} \frac{\sin^2[s_j(q-q_0)_y/2]}{\sin^2[(q-q_0)_y/2]} \times \frac{\sin^2[s_j(q-q_0)_z/2]}{\sin^2[(q-q_0)_z/2]} \simeq \sum_{\text{size } i} n_i s_i^6 e^{-s_i^2(q-q_0)^2/4\pi}$$
$$I(q) \simeq P(q-q_0, w, \langle s\rangle) e^{-\langle s\rangle^2(q-q_0)^2/[4\pi + w^2(q-q_0)^2]},$$
where
$$P(q-q_0, w, \langle s\rangle) = \frac{\langle s\rangle^3 \alpha^{-7/2}}{\left[1+\frac{3}{2}(w/\langle s\rangle)^2\right]} \left[\frac{15}{8}(w/\langle s\rangle)^6 + \frac{45}{4}(w/\langle s\rangle)^4\alpha^{-1} + \frac{15}{2}(w/\langle s\rangle)^2\alpha^{-2} + \alpha^{-3}\right]$$
with $\alpha = 1 + w^2(q-q_0)^2/4\pi$.
[25] For example, the size is reduced only by about 5.0% when $w/\langle s\rangle$ changes from zero to 0.3.

[26] We define the bulk lattice parameter of 2.996 Å as the distance between {100} lattice planes since bulk Tl has a hcp structure with lattice constants of a=3.46 Å and c=5.52 Å.

[27] Random spatial distribution of islands often causes diffuse scattering in the vicinity of specular direction. No such diffuse scattering observed in our measurements at small angles supports our assumption of large separation between islands.

[28] C. W. Mays, J. S. Vermaak, and D. Kuhlmann-Wilsdorf, Surf. Sci. **12**, 134 (1968); **12**, 128 (1968).